RESEARCH ARTICLE **ISSN 2738-9898 (Print) ISSN 2738-9901 (Online)**

H-infinity based modified droop control method for voltage and frequency regulation of an islanded microgrid supplying non-linear and unbalanced loads

Pramod Sharma[1,*], Ananta Adhikari [2], Sujan Khanal [1]

[1] Department of Electrical Engineering, IOE, Pashchimanchal Campus, Tribhuvan University, Pokhara, Nepal

[2] School of Engineering, Pokhara University, Kaski, Pokhara, Nepal

*Author to whom correspondence should be addressed; E-Mail: *pramodwrc070@gmail.com*

Received : 11 February 2025; Received in revised form : 22 March 2025; Accepted : 24 March 2025; Published: 04 July 2025

Abstract

This paper presents an advanced control method for islanded microgrid (MG) based on the H-infinity (H∞) controller. The proposed method is designed to regulate system voltage and frequency within acceptable ranges under disturbances caused by load variations. The method is also used to ensure equal power sharing by each voltage source inverters (VSIs). To evaluate its effectiveness, the proposed controller is compared with conventional droop controller. In this approach, the droop control loop, along with the current and voltage control loops, is optimized effectively to manage variations in the system load. The method incorporates repetitive control principles with internal model concept to achieve precise tracking of voltage and current errors. The proposed system model consists of three voltage source inverters (VSIs), linear, nonlinear and unbalanced loads. The performance and feasibility of the proposed method is evaluated through MATLAB/Simulink simulations, including FFT analysis for harmonic assessment. The Comparative analysis with the traditional droop control method demonstrates the superior performance of the proposed method in managing microgrid operation in islanded mode.

Keywords

H-infinity, Modified droop controller, Non-linear and unbalanced loads, Islanded microgrid

1. Introduction

A microgrid (MG) is a low-voltage distribution network that includes multiple distributed generators (DGs), energy storage systems and loads. It can function in either grid-connected mode or islanded mode. In the grid-connected mode, the microgrid can exchange power with the main utility grid based on its generation capacity and load demands, while the voltage and frequency are generally regulated within the grid's standard limits. In contrast, during islanded mode, the voltage and frequency may deviate from acceptable levels due to the lack of grid support. To ensure proper operation in islanded mode, a control system is essential for adjusting these parameters to their specified limits.

There are several control methods for regulating the voltage and frequency of islanded microgrid. These methods include master/slave control, hierarchical control, multi-agent

system (MAS) control and droop control. Master/Slave Control method for controlling voltage and frequency of microgrid is proposed in [1]. This method used one of the distributed generators (DGs) as the master unit, while the others operate as slave units. The study shows that this method relies heavily on communication systems between the controller units. The failure in the master unit could result in complete system failure.

The hierarchical control method for microgrids in grid connected and islanded mode is proposed in [2]. This method used three control level, they are primary, secondary, and tertiary control. The study highlights that this method is highly efficient but it is not cost-effective and may not be the most practical or suitable solution for remote or locally isolated microgrids.

The simple method used for controlling islanded microgrid is droop control method. This is widely used control technique to regulate the system's voltage and frequency in islanded operation. It provides reference values for voltage and frequency based on the power requirements of the microgrid.

The conventional droop control method, though widely used in islanded microgrids it has several limitations that hinder its overall performance. In larger or more complex systems, the droop controller may struggle to maintain system stability, particularly in the presence of nonlinear or unbalanced loads. These limitations emphasize the need for more advanced and adaptive control techniques to improve system performance and stability in islanded microgrid operations [3], [4].

A model predictive control method is proposed in [5]. This study highlights the use of model predictive control (MPC) method for smooth transition between grid-connected and islanded mode without significant voltage and current deviations caused by mismatches in phase, frequency or amplitude between grid voltage and load.

A voltage controller utilizing H-infinity and repetitive control techniques is proposed in [6]. The study highlights the design of voltage controller. It uses repetitive control based on the internal model principle. The repetitive control provides outstanding voltage tracking performance by effectively handling a wide range of harmonics simultaneously. This results in significantly reduced total harmonic distortion and enhanced tracking accuracy. The study shows that controller can be used in both islanded and grid connected mode.

A current control strategy is proposed in [7]. The study shows the design of current controller aiming to inject a clean sinusoidal current into the system even under nonlinear or unbalanced load conditions. The controller comprises an internal model and a stabilizing compensator design by H-infinity control theory.

A modified droop control method with H-infinity controller is proposed in this paper. The primary objective of this study is to improve the voltage and frequency of the microgrid supplying nonlinear and unbalanced loads. Additionally, the study aims to ensures the equal power sharing among each voltage source inverters (VSIs) and to minimize total harmonic distortion (THD) caused by non-linear loads, keeping it within acceptable limits.

2. Materials and Methods

2.1 General Outline of the Methodology

The proposed methodology involves the modeling and comparison of conventional droop control method with modified droop control method based on H-infinity controller. The overall process of methodology is shown Figure 1.

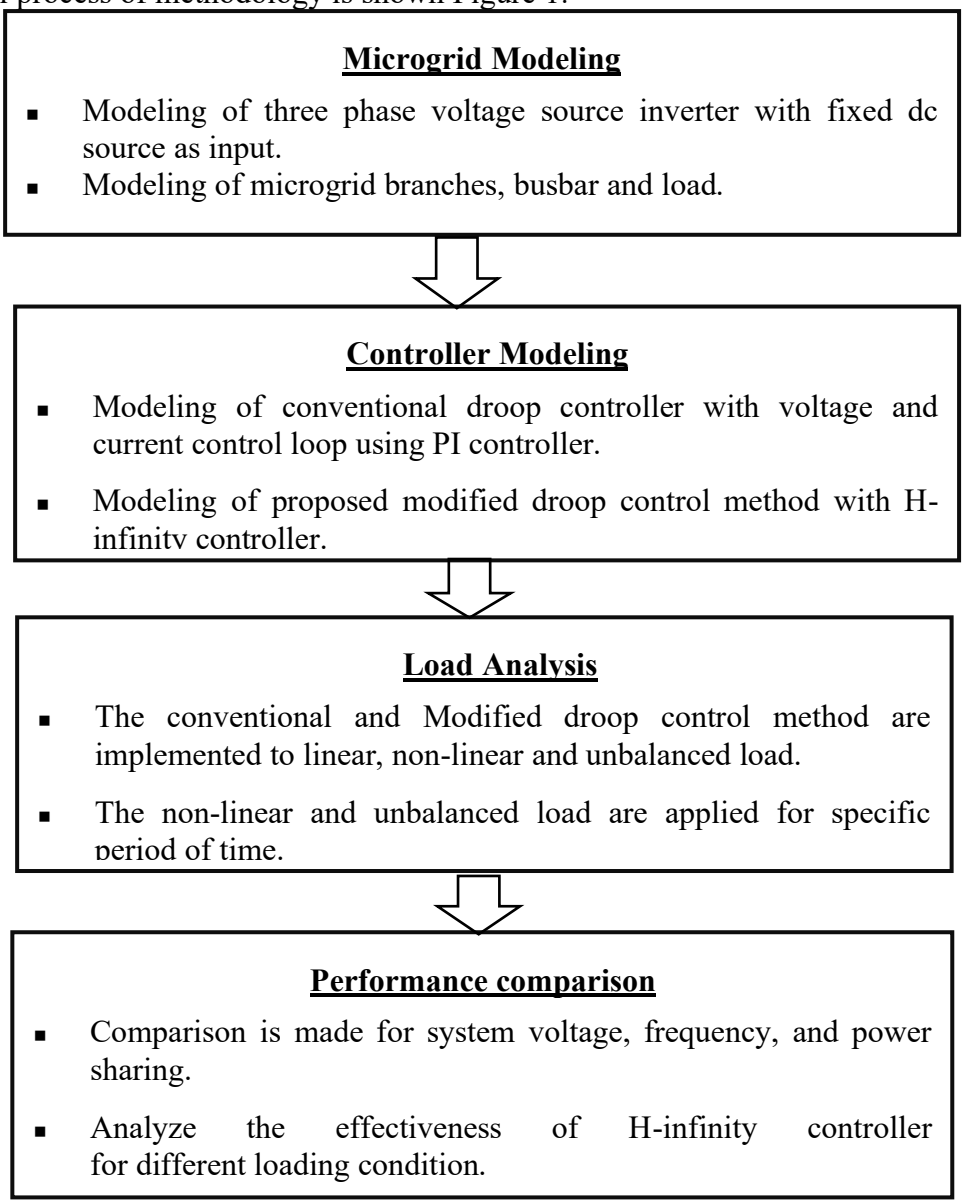

Figure 1: Overall Methodology

2.2 System Structure Model

It consists of three fixed dc source connected with separate VSI. Each VSI is connected to the common bus through LCL filters and supply linear, non-linear and unbalance load. The single line diagram of the microgrid adopted in this study is shown in Figure 2.

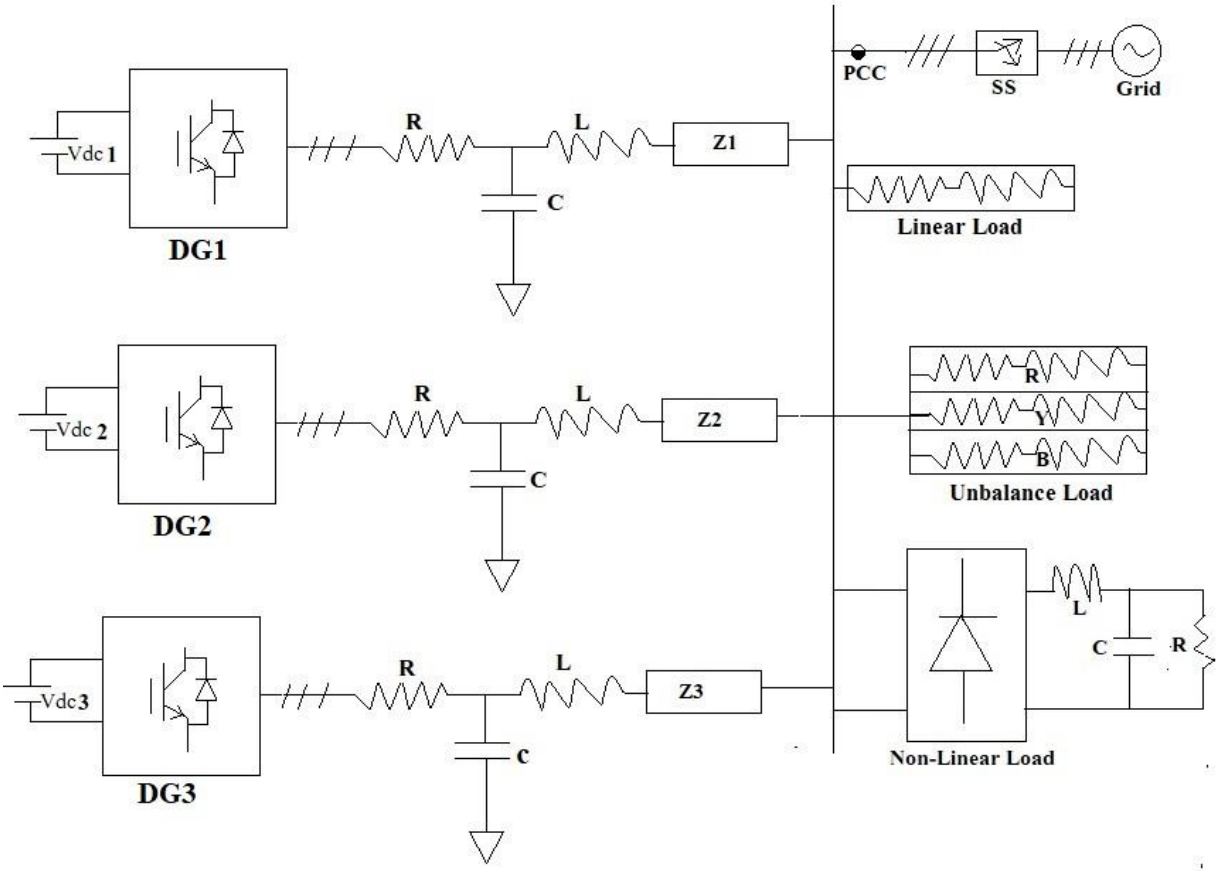

Figure 2: Single line diagram of micro grid system

2.3 Conventional Droop Control Method

The mathematical parameters used to model the conventional droop controller are explained below.

2.3.2 Droop Controller

The droop control method depends on the relationship between active power with frequency and reactive power with voltage. The droop control method can be expressed mathematically as [8].

$$\omega^* = \omega_{ref} - m_p \, P_{gi} \quad (1)$$

$$v^*_{od} = v_{ref} - n_p \, Q_{gi} \quad (2)$$

$$v^*_{oq} = 0 \quad (3)$$

Where ω_{ref} is the reference angular frequency, v_{ref} is the reference voltage, ω^* is the nominal angular frequency, v^*_{od} and v^*_{oq} are the d-axis and q-axis voltage and m_p and n_p are the droop coefficient.

2.3.3 Voltage Controller

The Voltage Controller Differential Algebraic Equations can be expressed as [3]:

$$\acute{\emptyset}_{qi} = V^*_{qi} - V_{qi} \quad (4)$$

$$\acute{\emptyset}_{di} = V^*_{di} - V_{di} \quad (5)$$

$$i^*_{ldi} = F_i i_{di} - \omega C_{fi} V_{qi} + K_{Pvi}(V^*_{di} - V_{di}) + K_{IVi}\acute{\emptyset}_{di} \quad (6)$$

$$i^*_{lqi} = F_i i_{qi} - \omega C_{fi} V_{di} + K_{Pvi}(V^*_{qi} - V_{qi}) + K_{IVi}\acute{\emptyset}_{qi} \quad (7)$$

Where $\emptyset_{qi}$ and $\emptyset_{di}$ are the state variable defined for PI controllers, K's are the integrator gain factors, F_i is the feed forward gain and ω is the nominal angular frequency.

2.3.4 Current Controller

The current controller Differential Algebraic Equations can be expressed as [3]:

$$\acute{\gamma}_{qi} = i^*_{lqi} - i_{lqi} \quad (8)$$

$$\acute{\gamma}_{di} = i^*_{ldi} - i_{ldi} \quad (9)$$

$$V^*_{idi} = -\omega L_{fi} i_{lqi} - K_{PCi}(i^*_{ldi} - i_{ldi}) + K_{ICi}\gamma_{di} \quad (10)$$

$$V^*_{iqi} = -\omega L_{fi} i_{ldi} - K_{PCi}(i^*_{lqi} - i_{lqi}) + K_{ICi}\gamma_{qi} \quad (11)$$

Where γ_{di} and γ_{qi} are the state variables defined for PI controllers, K's are the integrator gain factors, and i_{ldi} and i_{lqi} are the direct and quadrature components of . i_{li}

2.3.5 Control system diagram

The complete control system diagram of conventional droop control method is shown in Figure 3 [3].

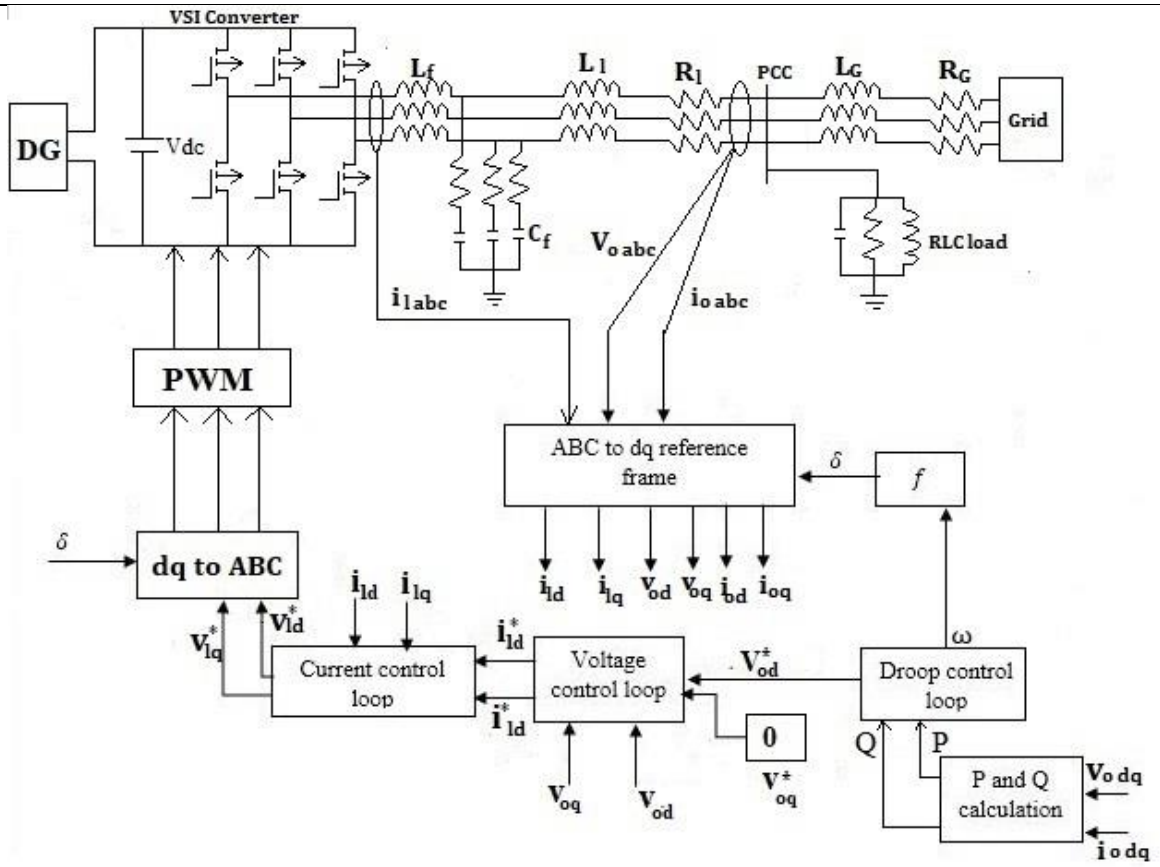

Figure 3: Complete control system of the conventional droop control method

2.4 Proposed Control Method

The traditional control method does not have the ability to adjust the system voltage and frequency to their nominal values after any variation in system load. Therefore, a supplementary control is needed to enhance the performance of traditional controller. This paper proposed an advanced control method based on H∞ controller.

2.4.1 Concept of H∞ Control

The H∞ control method is a very powerful technique in modern control theory. It provides robust stability for the linear multivariable systems in the presence of uncertainties and disturbances. The block diagram of the H∞ control method is shown in Figure 4 [6], where P represent the transfer function of the plant and C is the controller to be designed. Also, u represents the control input, w represents the disturbances and other external inputs, y represents the measured output, and z represents the controlled output. This control method is applied to reduce the mismatch between the generation and the load for MGs in islanded mode. It also adjusts the system voltage and frequency to their nominal values after system load variation.

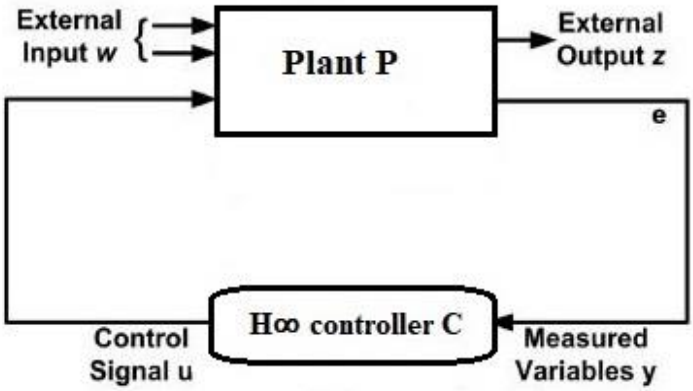

Figure : 4 Block diagram of H∞ controller

To improve the performance of the H∞ controller, an internal model M is used. It provides a repetitive control scheme to cover a wide range of frequencies. It consists of a low pass filter with a transfer function W(s) connected in feedback path with $e^{-T_d S}$ as shown in Figure 5 [6]. It is responsible for generating periodic signals of a given fundamental period, T_d, therefore, it has the ability to track periodic references and reject periodic disturbances having the same period. The transfer function of low pass filter and expression for delay time can be obtain as [9]:

$$W(s) = \frac{\omega_c}{s + \omega_c} \tag{12}$$

$$T_d = T - \frac{1}{\omega_c} \tag{13}$$

Where ω_c is the cut-off frequency of the low pass filter W(s) and T is the fundamental period.

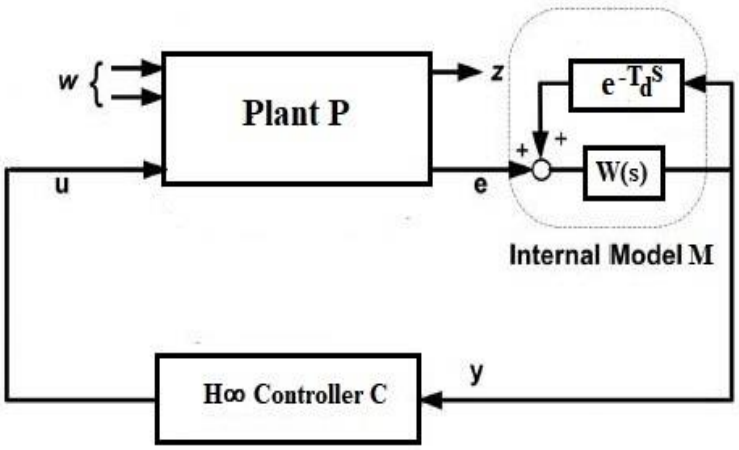

Figure 5: Block diagram of H∞ repetitive controller

To ensure the system stability, two weighting parameters ξ and μ are incorporated after opening the local feedback loop of internal model as shown in Figure 6 [6]. The additional parameters ξ and μ provide more freedom in the design.

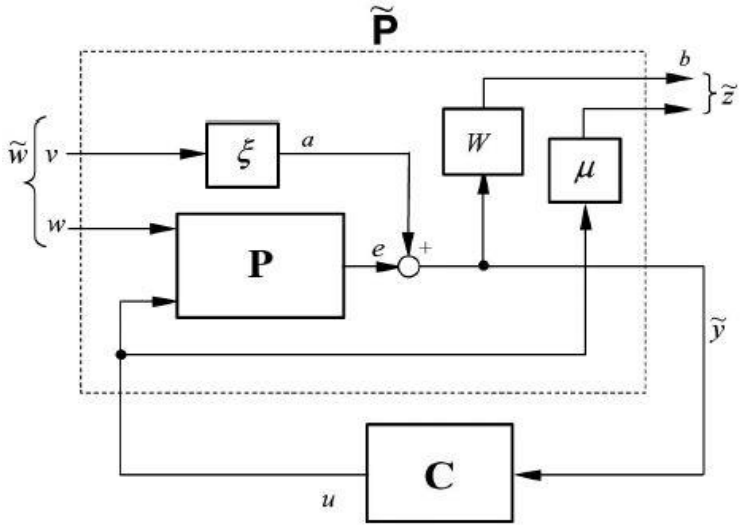

Figure 6: Block diagram of H∞ repetitive controller with weighting parameters

2.4.2 Overall control system

The proposed H∞ control method consists of three control loop: power control loop, voltage control loop and current control loop. The power control loop is used to generate the reference voltage and frequency, as well as to ensure accurate active and reactive power sharing between the connected DGs. Similarly, the voltage control loop generates the reference current signal for the current control loop and the current control loop generates the reference voltage signal for the VSI. The complete control system of proposed control method is shown in Figure 7 [10].

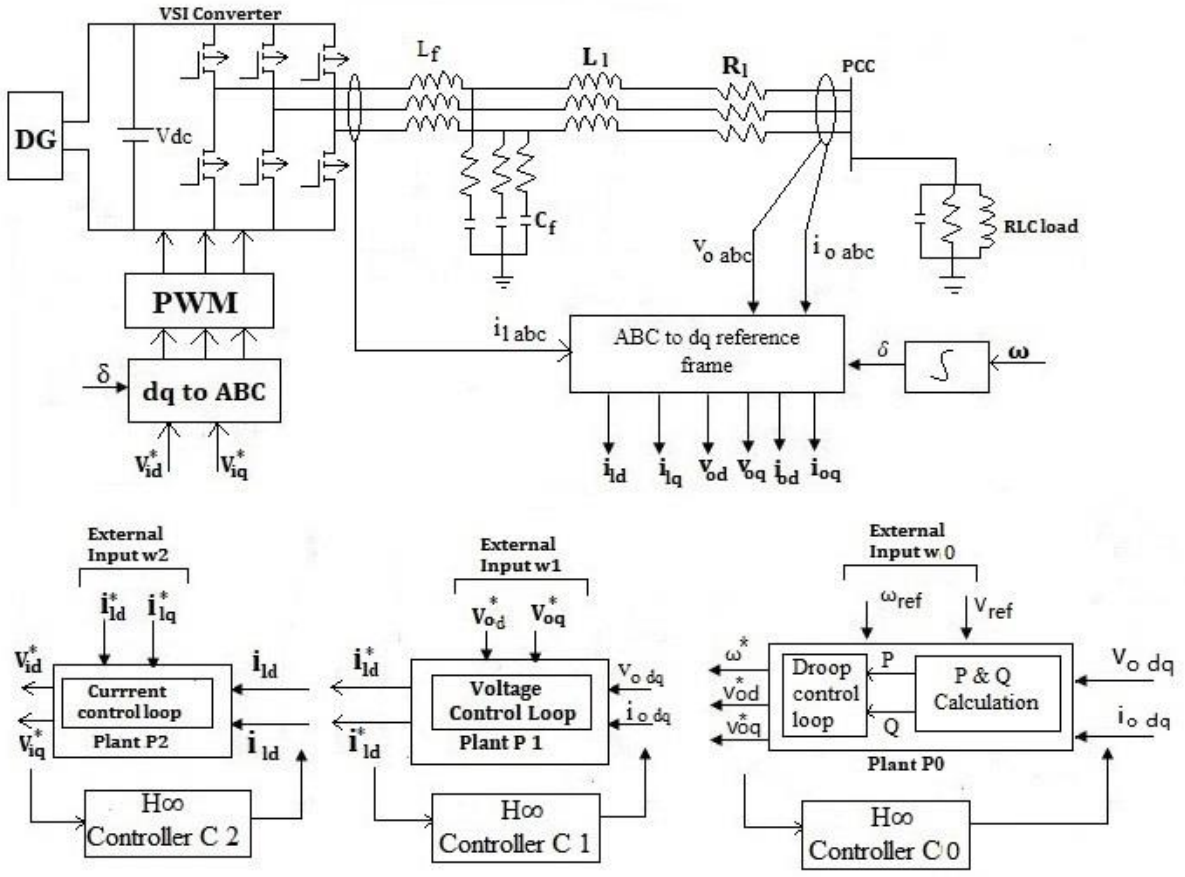

Figure 7: Complete control system of H∞ control method

2.4.2.1 Power control loop

The power control loop consists of a power calculation and a droop controller, and in this loop, the H∞ control method is applied to compensate the difference between the measured and the reference values of the active and reactive power to ensure accurate power sharing between the connected DGs. The state space modeling of power control loop can be expressed as [6],[10].

$$\dot{x}_p = A_p x_p + B_{p1} w_p + B_{p2} u_p \quad (14)$$

$$\dot{y}_v = C_p x_p + D_{p1} w_p + D_{p2} u_p \quad (15)$$

The corresponding plant transfer function can be represented as:

$$P_0 = [D_{pi1} \quad D_{pi2}] + C_{pi}(sI - A_{pi})^{-1}[B_{pi1} \quad B_{pi2}] \quad (16)$$

To provider repetitive control a low pass filter $W_0(s)$ having cut off frequency $\omega_{c0}$is integrated with a delay line $e^{-T_d s}$. To improve the system stability, the original plant P_0 is generalized to $\widetilde{P}_0$. The generalized plant $\widetilde{P}_0$ includes the original plant P_0, low pass

filter$W_0(s)$and controller weighted parameters ξ_0 and μ_0. The generalized plant can be expressed as:

$$\tilde{P}_0 = \begin{bmatrix} A_{pi} & 0 & 0 & B_{pi1} & B_{pi2} \\ B_{w0}C_{pi} & A_{w0} & B_{w0}\xi_0 & B_{w0}D_{pi1} & B_{w0}D_{pi2} \\ D_{w0}C_{pi} & C_{w0} & D_{w0}\xi_1 & D_{w0}D_{pi1} & D_{w0}D_{pi2} \\ 0 & 0 & 0 & 0 & \mu_0 \\ C_{pi} & 0 & \xi_0 & D_{pi1} & D_{pi2} \end{bmatrix} \quad (17)$$

2.4.2.2 Voltage and current control loop

The voltage control loop consists of plant P1 and a stabilizing compensator C1. The model of the plant P1 is derived using single phase diagram shown in Figure 8 [6].

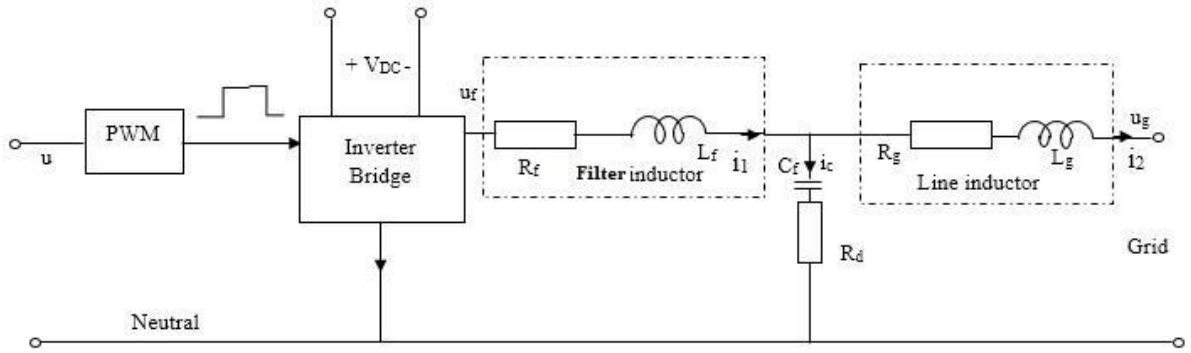

Figure 8: Single phase representation of the plant

The current of the inductors and the voltage of the capacitor are chosen as state variables $x_v=[i_1, i_2, u_c]^T$. The external input $w_v=[u_c, u_{ref}]^T$ consists of the capacitor voltage u_c and the reference voltage u_{ref}, and the control input u_v. The plant P_1 can then be described by the state equation as follow [6], [7].

$$\dot{x}_v = A_v x_v + B_{v1} w_v + B_{v2} u_v \quad (18)$$

$$\dot{y}_v = C_v x_v + D_{v1} w_v + D_{v2} u_v \quad (19)$$

The corresponding plant transfer function can be represented as:

$$P_1 = [D_{v1} \quad D_{v2}] + C_v(sI - A_v)^{-1}[B_{v1} \quad B_{v2}] \quad (20)$$

To provider repetitive control a low pass filter $W_1(s)$having cut off frequency $\omega_{c1}$is integrated with a delay line $e^{-T_d s}$. To improve the system stability, the original plant P_1 is generalized to $\tilde{P}_1$. The generalized plant $\tilde{P}_1$ includes the original plant P_1, low pass filter $W_1(s)$ and controller weighted parameters ξ_1 and μ_1. The generalized plant can be expressed as [6], [11].

$$\tilde{P}_1 = \begin{bmatrix} A_v & 0 & 0 & B_{v1} & B_{v2} \\ B_{w1}C_v & A_{w1} & B_{w1}\xi_1 & B_{w1}D_{v1} & B_{w1}D_{v2} \\ D_{w1}C_v & C_{w1} & D_{w1}\xi_1 & D_{w1}D_{v1} & D_{w1}D_{v2} \\ 0 & 0 & 0 & 0 & \mu_1 \\ C_v & 0 & \xi_1 & D_{v1} & D_{v2} \end{bmatrix} \quad (21)$$

Similarly, plant $\tilde{P}_2$ for current controller can be determine and expressed as[7], [12].

$$\tilde{P}_2 = \begin{bmatrix} A_i & 0 & 0 & B_{i1} & B_{i2} \\ B_{w1}C_i & A_{w2} & B_{w2}\xi_2 & B_{w2}D_{i1} & B_{w2}D_{i2} \\ D_{w2}C_i & C_{w2} & D_{w2}\xi_2 & D_{w2}D_{i1} & D_{w2}D_{i2} \\ 0 & 0 & 0 & 0 & \mu_2 \\ C_i & 0 & \xi_2 & D_{v1} & D_{i2} \end{bmatrix} \quad (22)$$

Based on plant $\tilde{P}_0$, $\tilde{P}_1$ and $\tilde{P}_2$ the controller C0, C1 and C2 are designed in the MATLAB using hinfsyn function. Once the controller C0, C1, and C2 are designed these are integrated with droop control loop, voltage control loop and current control loop of conventional control method respectively.

3. Results and Discussions

3.1 Simulation and result

MATLAB simulation is performed for both conventional droop control method and modified droop control method. The system performance and output is checked for linear, non-linear and unbalance load. The overall simulation model for proposed system is shown in Figure 9.

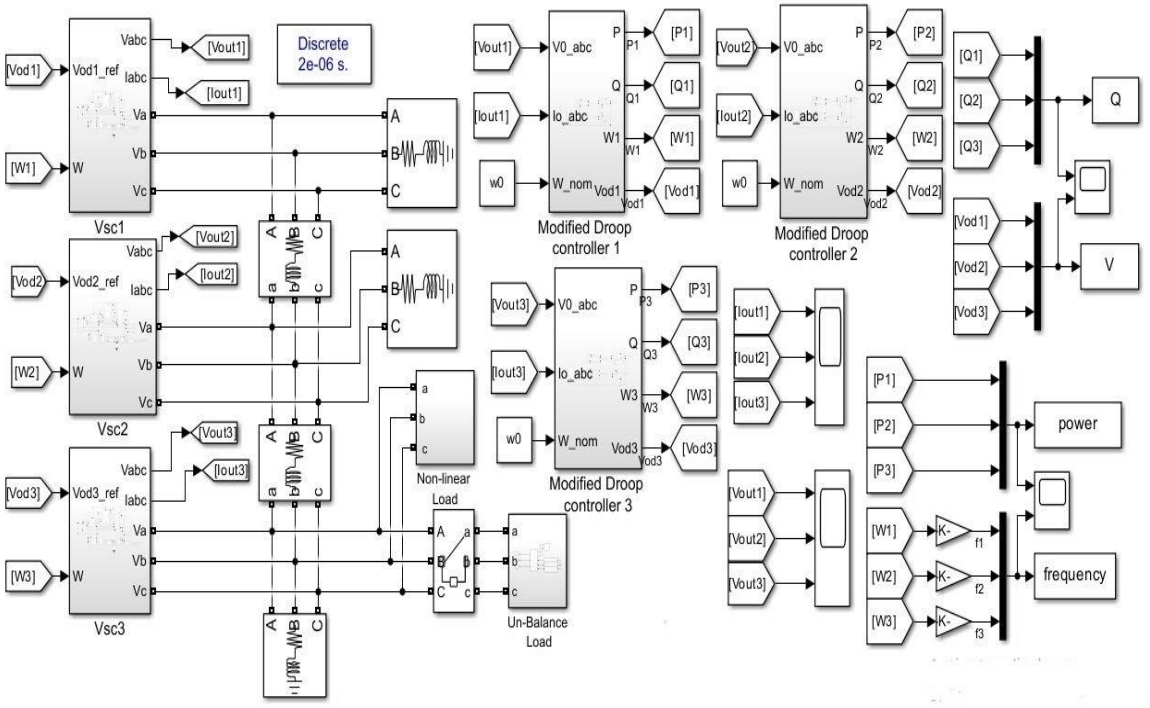

Figure 9: Overall simulation model

3.2 System Parameters

The different parameters used for simulation of proposed controller are shown in table below. The electrical parameters are present in Table 1. These include system frequency, resistance, inductance etc.

Table 1: Electrical system parameters

Components	Parameters	Symbol	Value	Units
DG system	Nominal frequency	ω^*	2Π*50	rad/s
	Nominal RMS voltage	V	380	volt
	DC voltage	V_{dc}	700	V
	PWM switching frequency	f_s	10	kHz
Converter LC filter	Series resistance	R_f	0.05	Ω
	Inductance	L_f	1.6	mH
	Capacitance	C_f	24	µF
	Shunt resistance	R_d	1.2	Ω
Droop Controller coefficient	Frequency droop	m_p	0.000005	
	Voltage droop	n_p	0.003	
Line parameters	Series resistance	R_g	0.140	Ω
	Inductance	L_g	0.5	mH

The power, voltage and current controller parameters are present in Table 2. These includes gain parameters, weighted parameters and delay time.

Table 2: Power, Voltage and current controller parameters

Components	Parameters	Symbol	Value	Units
Power controller(C0)	Weighted parameters	μ_0	0.65	
		ξ_0	3.2	
	Delay time	T_d	20	ms
Voltage controller(C1)	Proportional gain	K_{pv}	0.29	
	Integral gain	K_{iv}	594.9	
	Delay time	T_d	20	ms
		μ_1	0.85	
		ξ_1	2.6	
Current controller(C2)	Proportional gain	K_{pc}	55	
	Integral gain	K_{ic}	1570.9	
	Delay time	T_d	20	ms
	Weighted parameters	μ_2	0.27	
		ξ_2	100	

The active and reactive power demand of the load are present in Table 3. These includes linear balanced load, non-linear and unbalanced load

Table 3: Types of load and load demand used for simulation

Load Type	Symbol	Starting Load	Load addition At t=1 sec	Load Removed After t=2 sec	Load Removed After t=3 sec
Balanced Load	P1+Q1	20200 W + 1600 VAR	5800 W + 200 VAR	5800 W + 200 VAR	-
Non-linear load	P2+Q2	-	6000 W + 200 VAR	-	6000 W + 200 VAR
Unbalanced load	P3R+Q3R	-	600W+ 100VAR	-	600W+ 100VAR
	P3Y+Q3Y	-	1000W+ 120VAR	-	1000W+ 120VAR
	P3B+Q3B	-	2000W+ 150VAR	-	2000W+ 150VAR

3.3 Response of conventional droop control method for linear balanced load

3.3.1 Active Power Sharing

Figure 10 shows the active power shared by three VSI. Up to 1 second, each VSI is sharing the active power of 6733 watt. At t=1sec, a load of 5800 watt is added to the system and power shared by each VSI also increased correspondingly. At t=2sec, load of 5800 watt is removed from the system and the power shared by each VSI also decreased with equal amount.

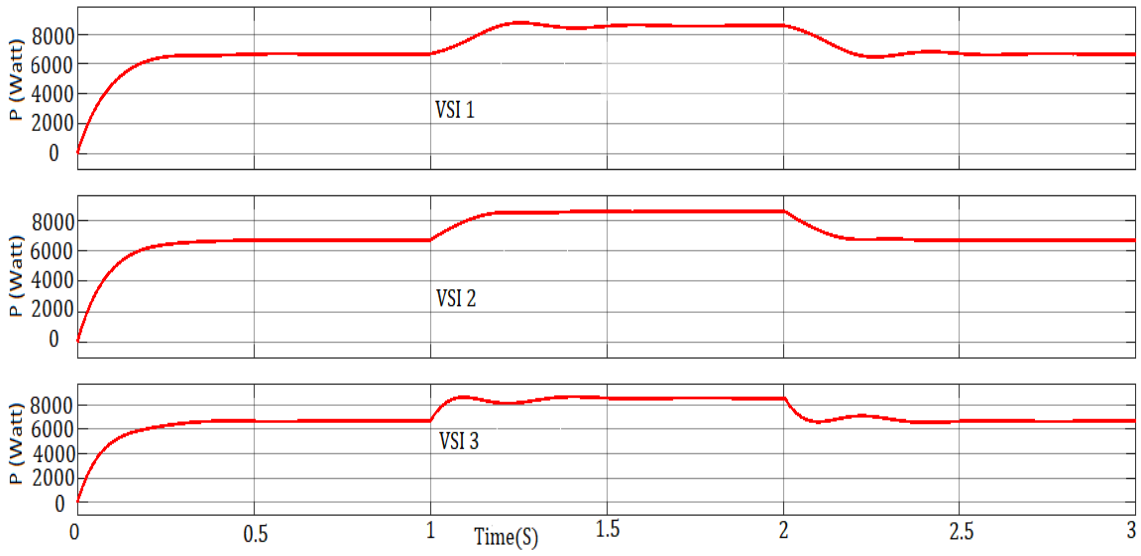

Figure 10: Active Power sharing

3.3.2 Reactive Power Sharing

Figure 11 shows the reactive power shared by three VSI. Up to 1 second, each VSI is sharing the reactive power of 566 VAR. At t =1sec, a load of 200 VAR is added and the reactive power shared by each VSI also increased correspondingly. At t=2sec, load of 200 VAR is removed from the system and the reactive power shared by each VSI also decreased with equal amount.

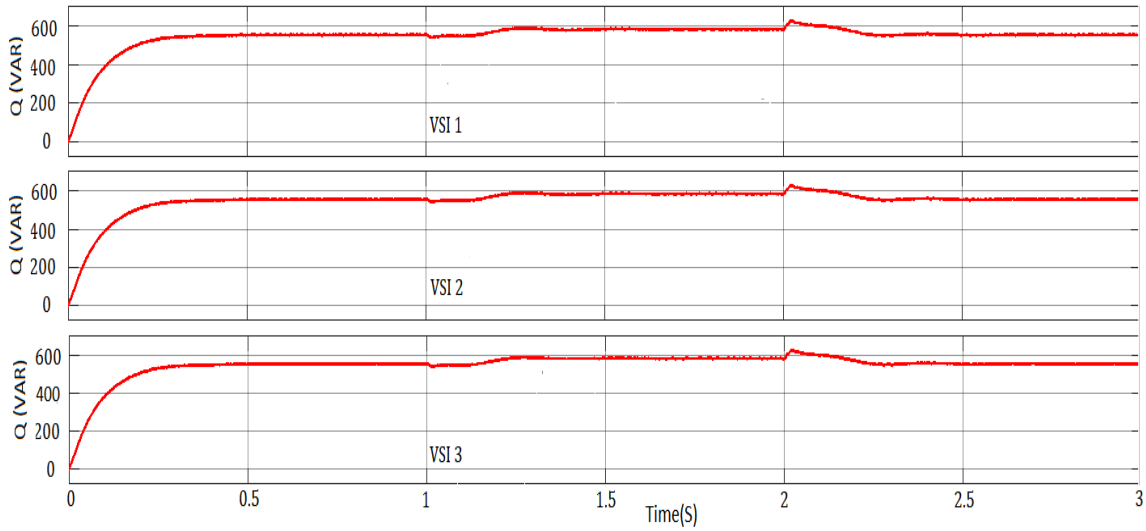

Figure 11: Reactive power sharing

3.3.3 System Voltage

For the balanced load, the output voltage waveform of all the VSI is sinusoidal, as shown in Figure 12.

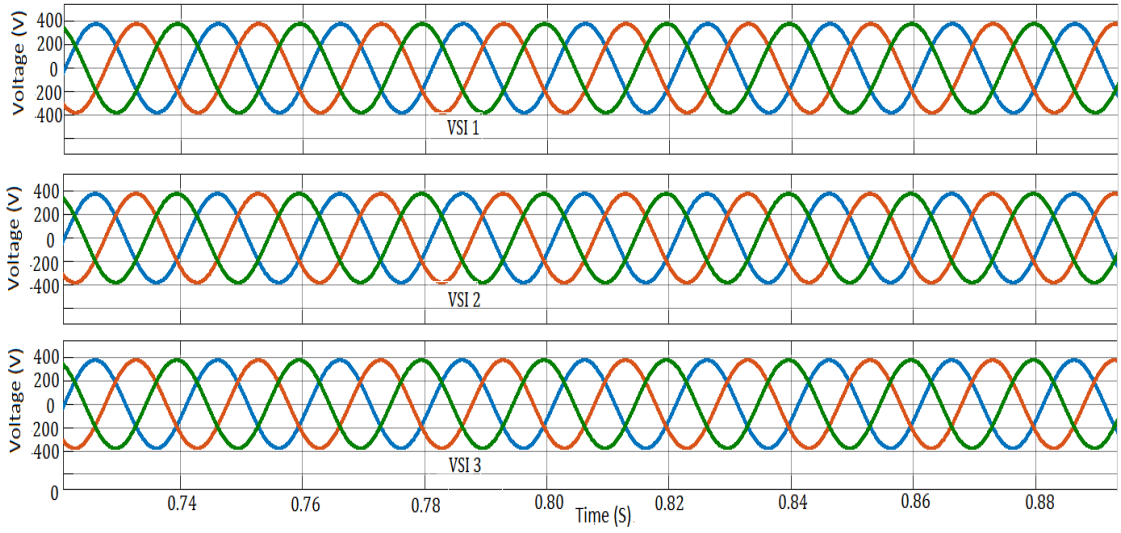

Figure 12: Voltage waveform

3.3.4 System frequency

The change in frequency to meet the system's active power demand remains within the limit as shown in Figure 13.

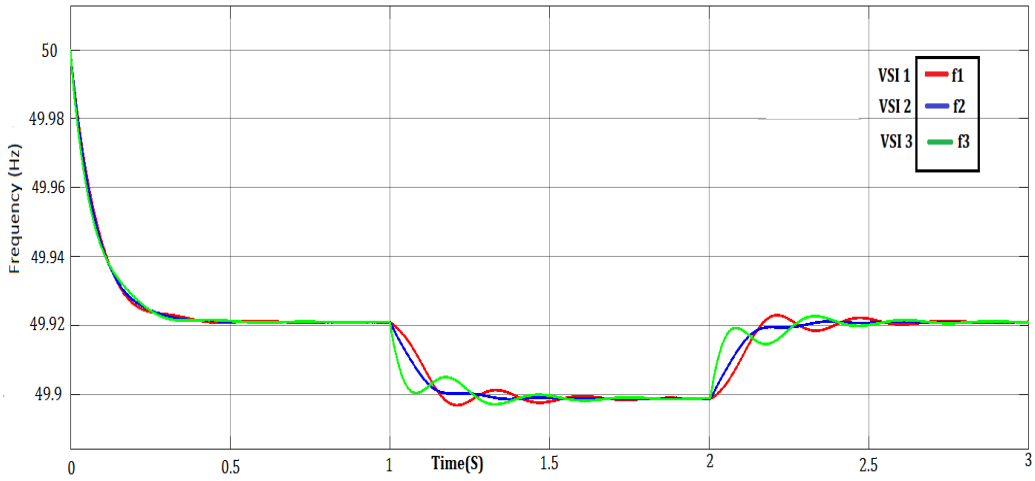

Figure 13: System frequency

3.4 Response of conventional droop control method for non-linear and unbalanced load

3.4.1 Active Power Sharing

Figure 14 shows the active power shared by three VSI. At t=1 sec, a non-linear and unbalanced load of 10 Kilowatt is added to the system. Due to unbalanced load each VSI shared the unequal power. At t=3sec, the load of 10 Kilowatt is removed and each VSI again shared equal amount of power.

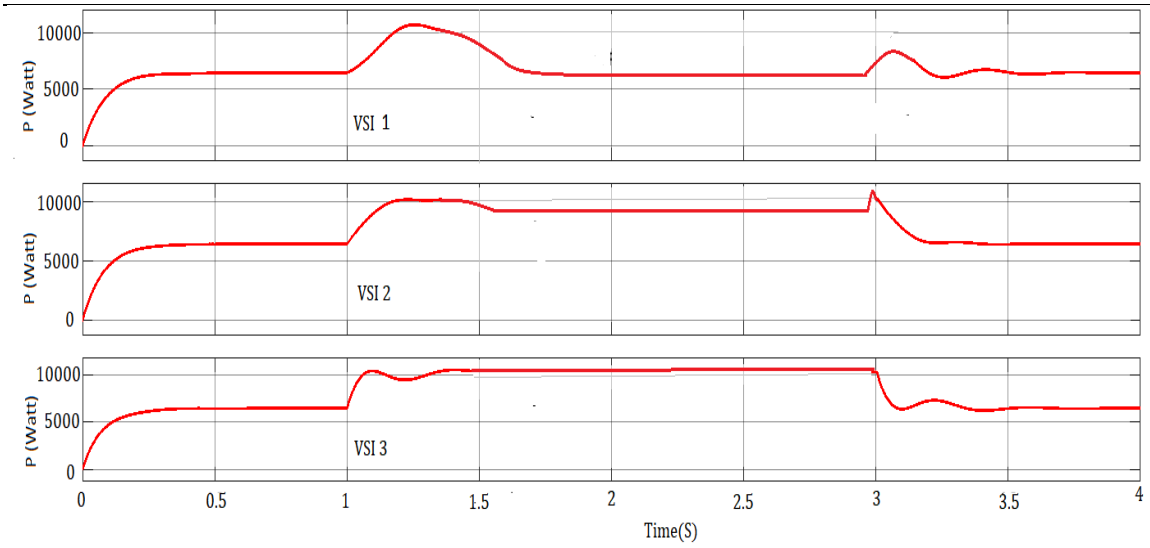

Figure 14: Active Power sharing

3.4.2 Reactive Power Sharing

Figure 15 shows the reactive power shared by three VSI. At t=1sec, a non-linear and unbalanced load of 570 VAR is added to the system. Due to unbalanced load each VSI shared unequal reactive power. At t=3sec, a non-linear and unbalance load is removed from the system and each VSI again shared equal amount of power.

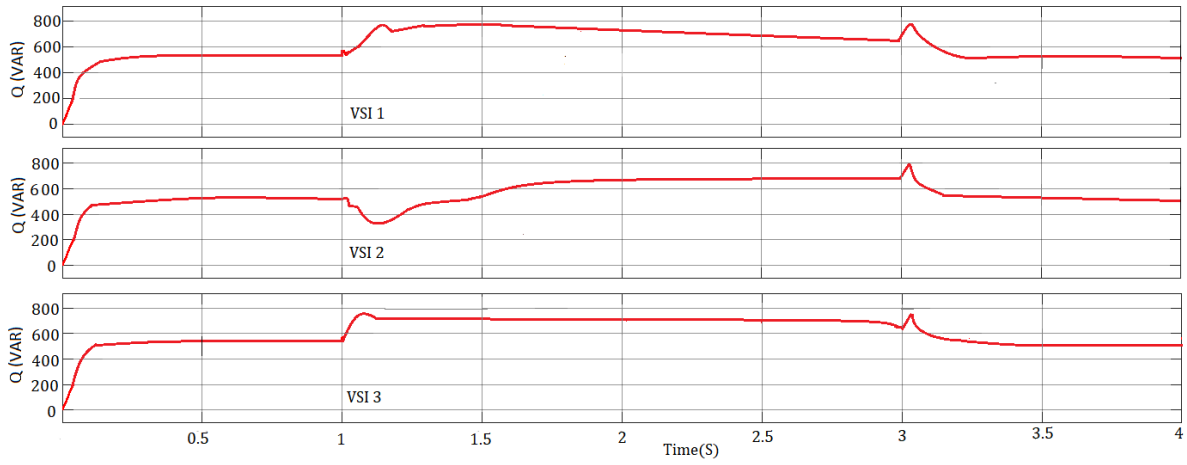

Figure 15: Reactive Power sharing

3.4.3 System Voltage

Figure 16 shows the load voltage waveform. At t=1sec, a non-linear and unbalanced load is added to the system. Due to non-linear and unbalanced load the voltage fluctuate with unequal magnitude in each phase. At t=3sec, nonlinear and unbalanced load is removed and the load voltage return to its original state.

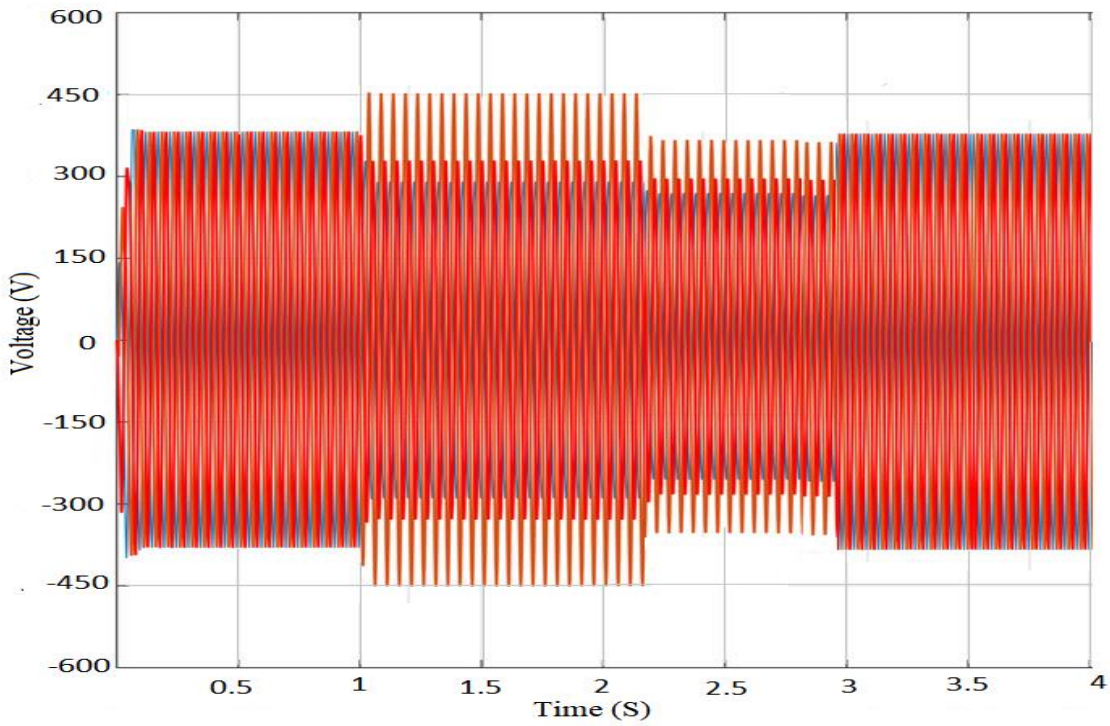

Figure 16: Voltage waveform due to non-linear and unbalanced load

3.4.4 System frequency

Up to 1 second, the system is supplying linear balanced load so the system frequency decreases with equal magnitude in each VSI. At t=1sec, a non-linear and unbalanced load is added to the system. Due to the presence of non-linear and unbalanced load the frequency of the system decrease with unequal magnitude as shown in Figure 17.

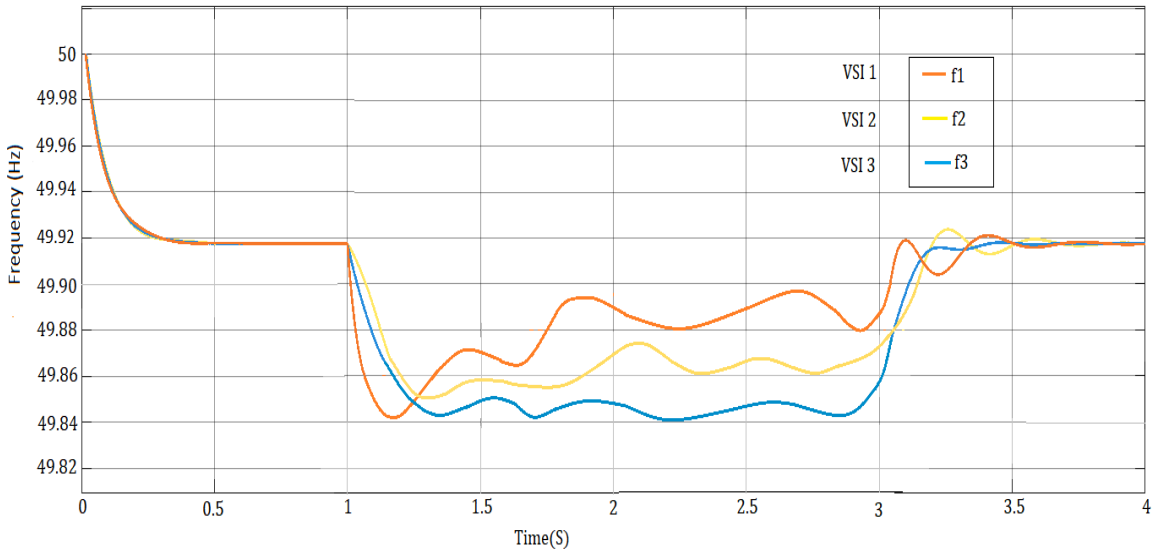

Figure 17: System frequency

3.4.5 Measure of Harmonic

The harmonic analysis of the inverter output voltage and current is done using MATLAB/FFT. The total harmonic distortion (THD) present in the current waveform due to

non-linear and unbalanced load is 17.13% (>5%) which is violating the standard limit as shown in Figure 18.

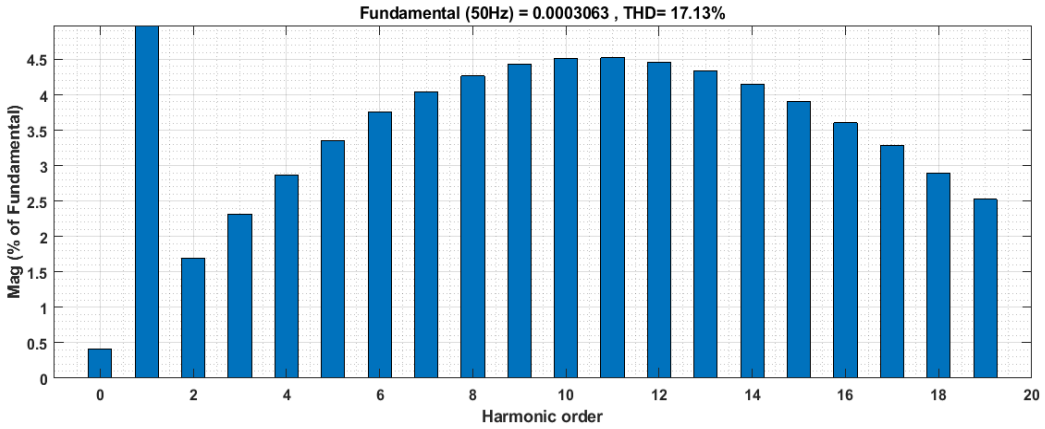

Figure 18: Total harmonic distortion (THD) in current waveform

The total harmonic distortion (THD) present in the voltage waveform due to non-linear and unbalanced load is 23.42% (>5%) which is also violating the standard limit as shown in Figure 19.

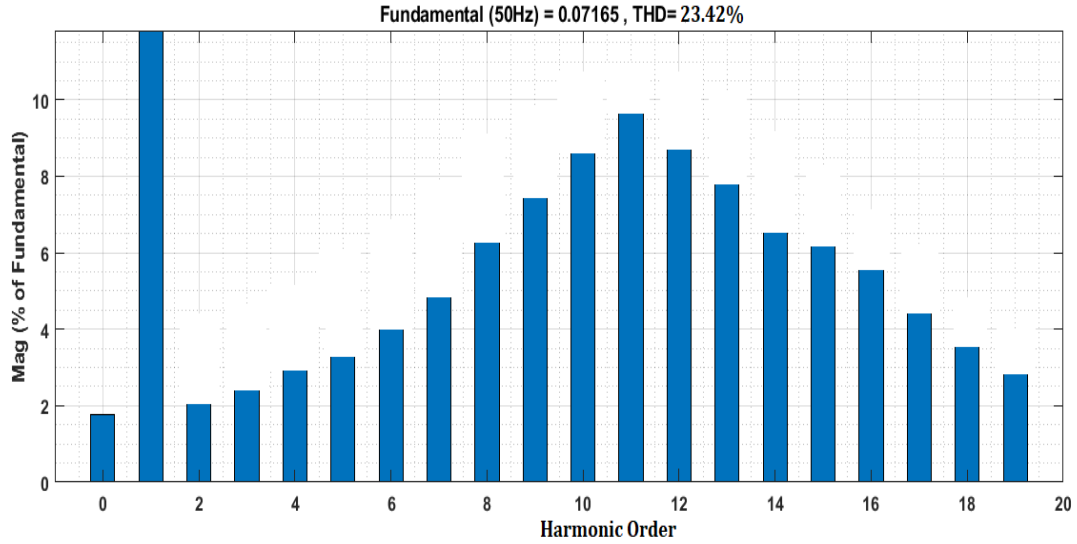

Figure 19: Total harmonic distortion (THD) in voltage waveform

3.5 Response of modified droop control method for non-linear and unbalanced load

3.5.1 Active Power Sharing

Figure 20 shows the active power shared by three VSI. Up to 1second each VSI is sharing the active power of 6733 watt. At t=1sec, a non-linear and unbalanced load of 10 Kilowatt is added to the system. The proposed H-infinity controller adjust the system frequency in such a way that each VSI share equal amount of power.

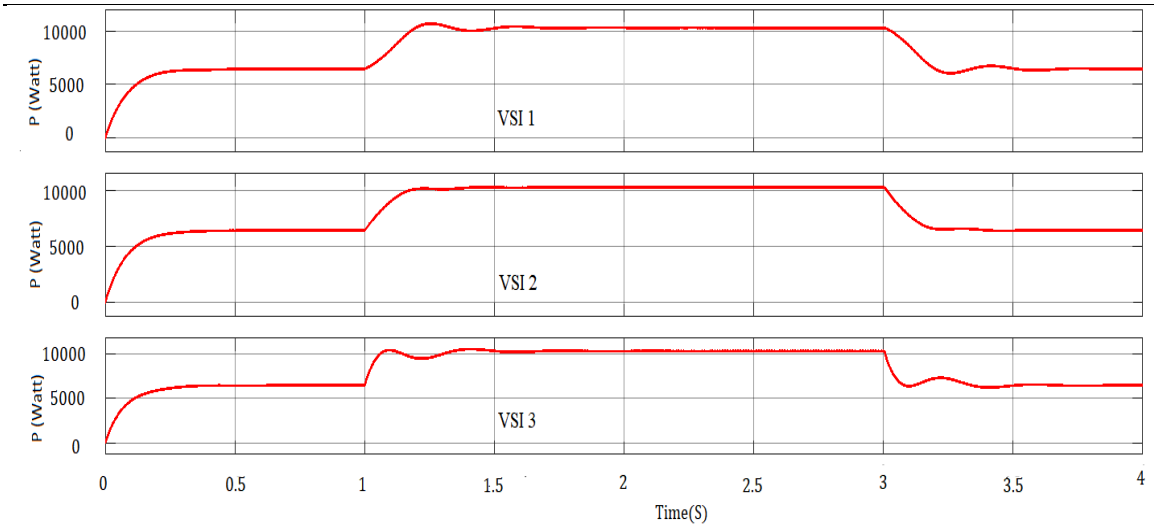

Figure 20: Active Power sharing

3.5.2 Reactive Power Sharing

Figure 21 shows the reactive power shared by three VSI. Up to 1 second each VSI is sharing the reactive power of 566 VAR. At t=1sec, a non-linear and unbalanced load of 570 VAR is added to the system. The proposed H-infinity controller adjust the system voltage in such a way that each VSI share equal amount of power.

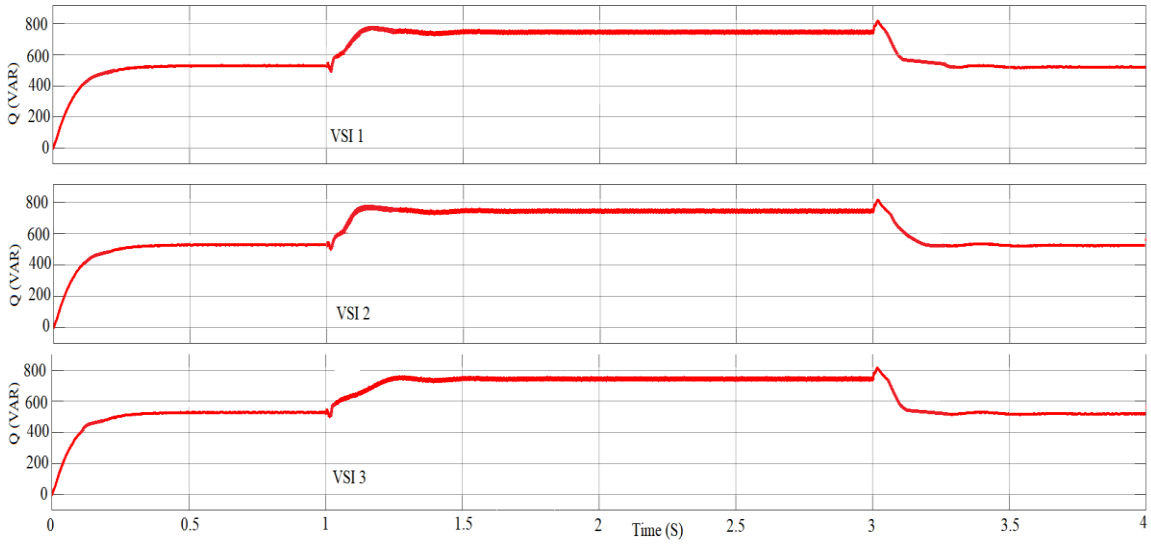

Figure 21: Reactive Power sharing

3.5.3 System Voltage

The voltage waveform due to non-linear and unbalanced load is shown in Figure 22. The proposed H-infinity controller adjust the waveform of output voltage and reduced the fluctuation in voltage. The voltage fluctuation reduced to 400V from 450V.

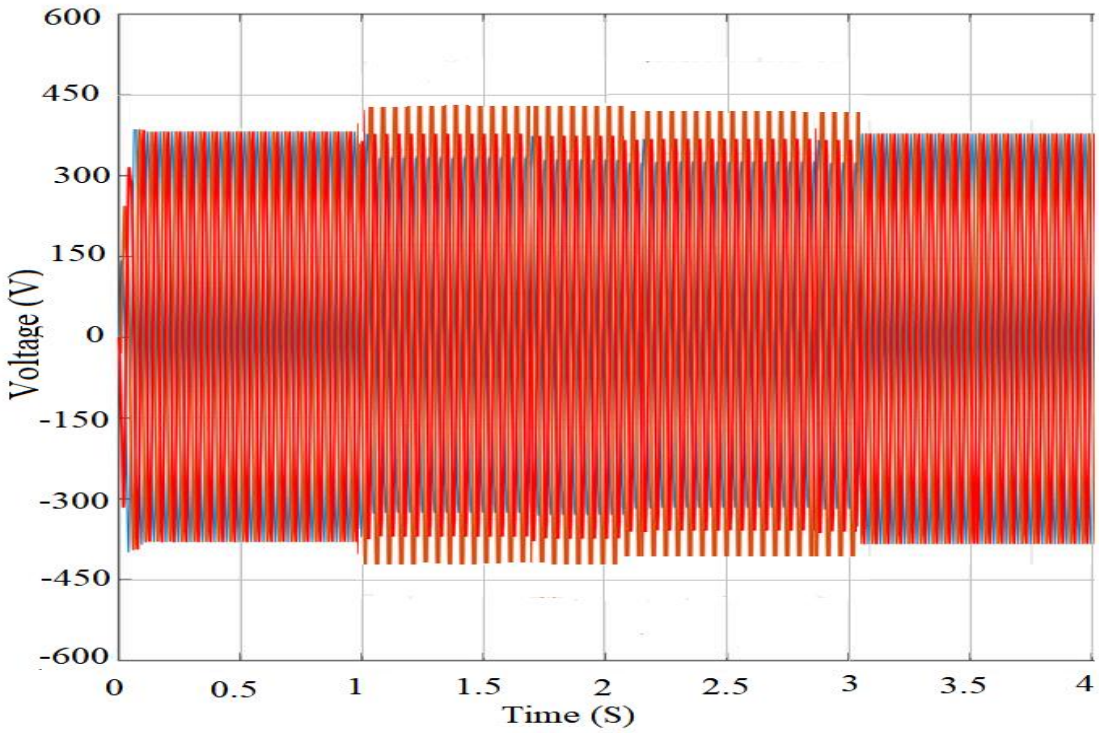

Figure 22: Voltage waveform due to non-linear and unbalanced load

3.5.4 System frequency

The proposed controller adjust the controller parameter in such a way that even in the presence of non-linear and unbalanced load the frequency of system is equally decreased in each VSI to supply the additional load. The decrease in frequency is within the limit as shown in Figure 23.

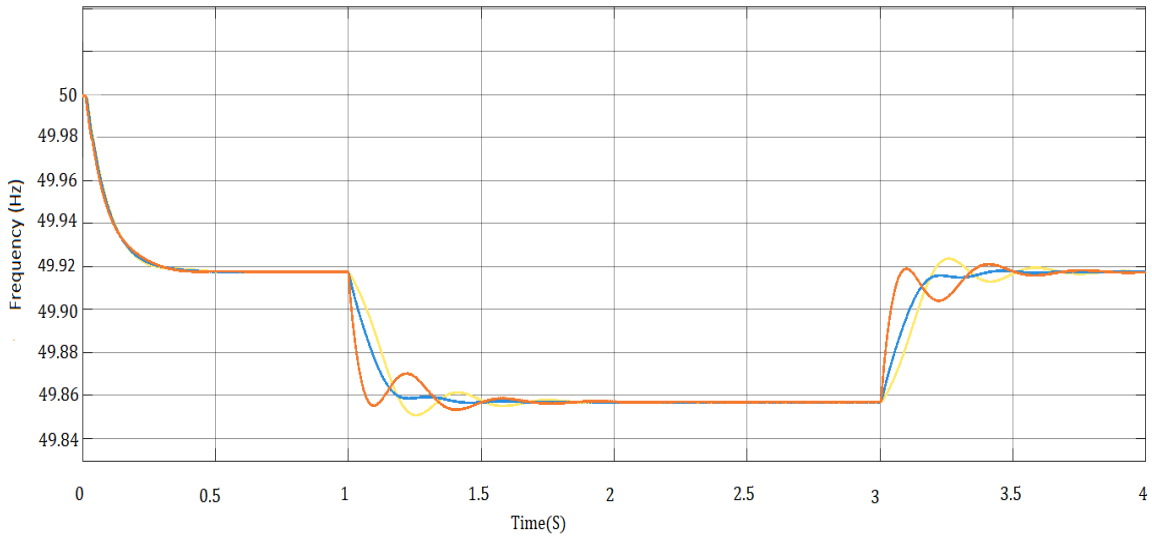

Figure 23: System frequency

3.5.5 Measure of Harmonic

The total harmonic distortion (THD) present in the current waveform due to non-linear and unbalanced load is 3.50% which is within the standard limit (<5%) as shown in Figure 24.

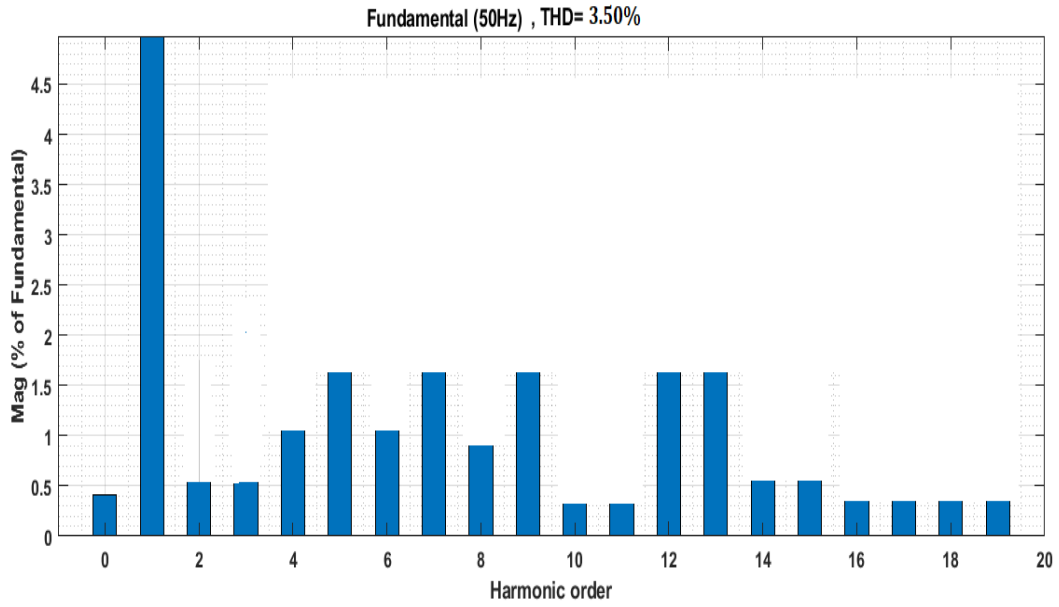

Figure 24: Total harmonic distortion (THD) in current waveform

The total harmonic distortion (THD) present in the voltage waveform due to non-linear and unbalanced load is 4.35% which is within the standard limit (<5%) as shown in Figure 25.

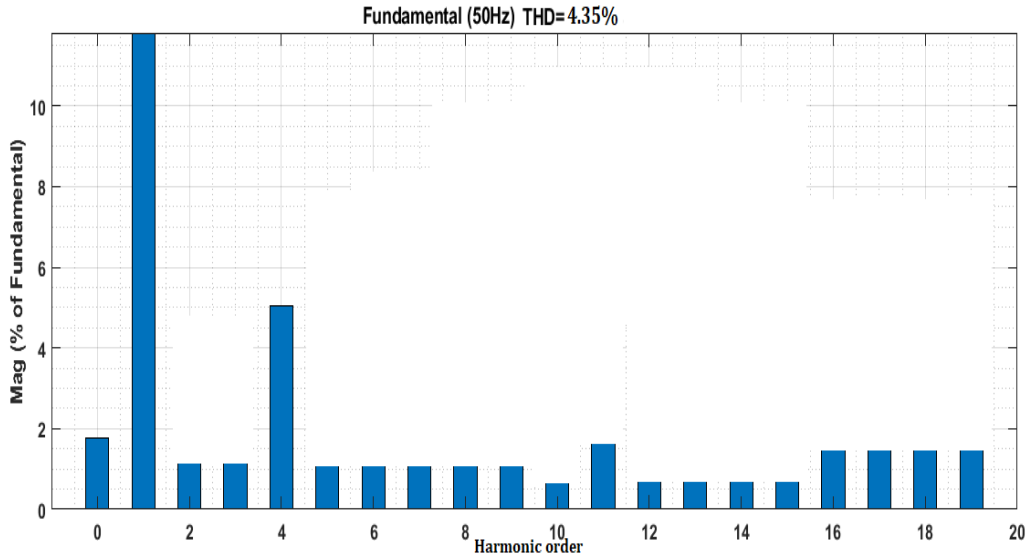

Figure 25: Total harmonic distortion (THD) in voltage waveform

3.6 Robustness analysis of proposed controller

To analyze the robustness of the proposed controller, the system is tested under varying load conditions. First, the load is increased beyond its normal operating value, and the active and reactive power shared by each VSI are observed. The analysis is then repeated for a decreased load condition.

3.6.1 With increased load

The proposed system is run for the load of active power 29800 watt and reactive power of 2170 VAR. To check the robustness, system load is increased by 3000 watt and 230 VAR.

The load is increased for t=1 to 3 second. From Figure 26, it is clear that each VSI is sharing equal active power of 10933 watt for increased in active power demand.

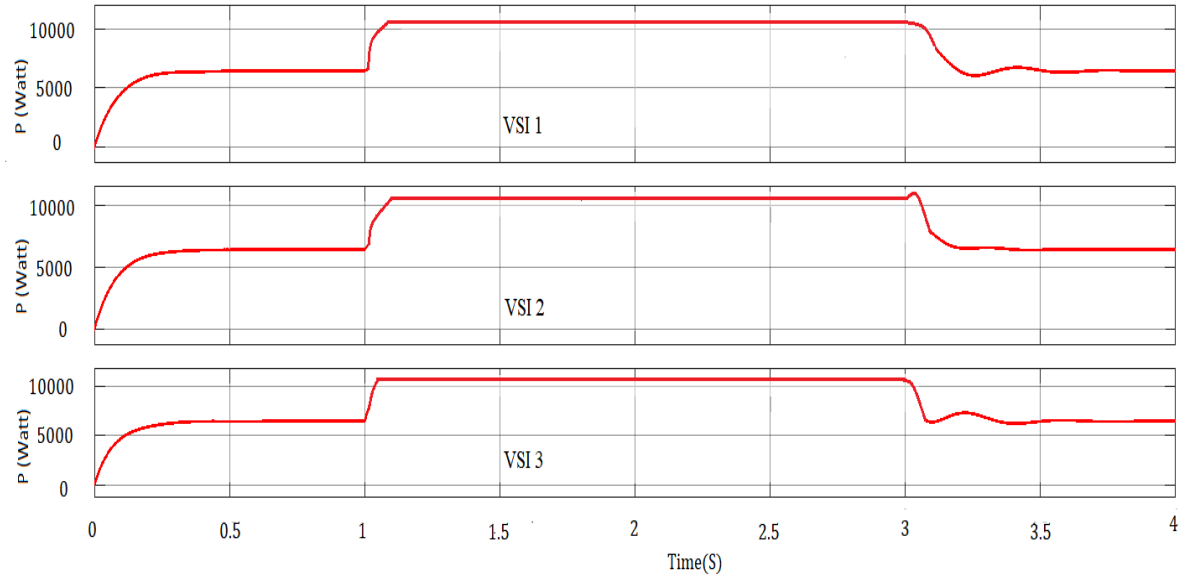

Figure 26: Active Power shared by VSI

Also, from Figure 27, it is clear that VSI is sharing equal reactive power of 800 VAR for increased in reactive power demand.

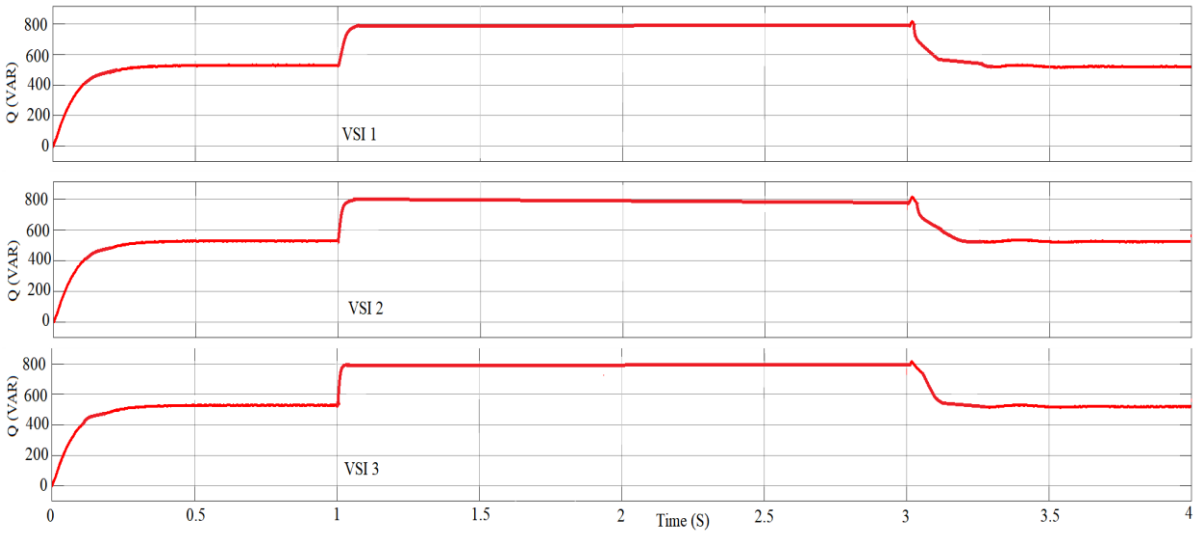

Figure 27: Reactive Power sharing by three VSI

3.6.2 With reduced load

To check the robustness for reduced load condition, system load is decreased by 2800 watt and 370 VAR. The load is decreased for t=1 to 3 second. From Figure 28, it is clear that each VSI is sharing equal active power of 9000 watt for decreased in active power demand.

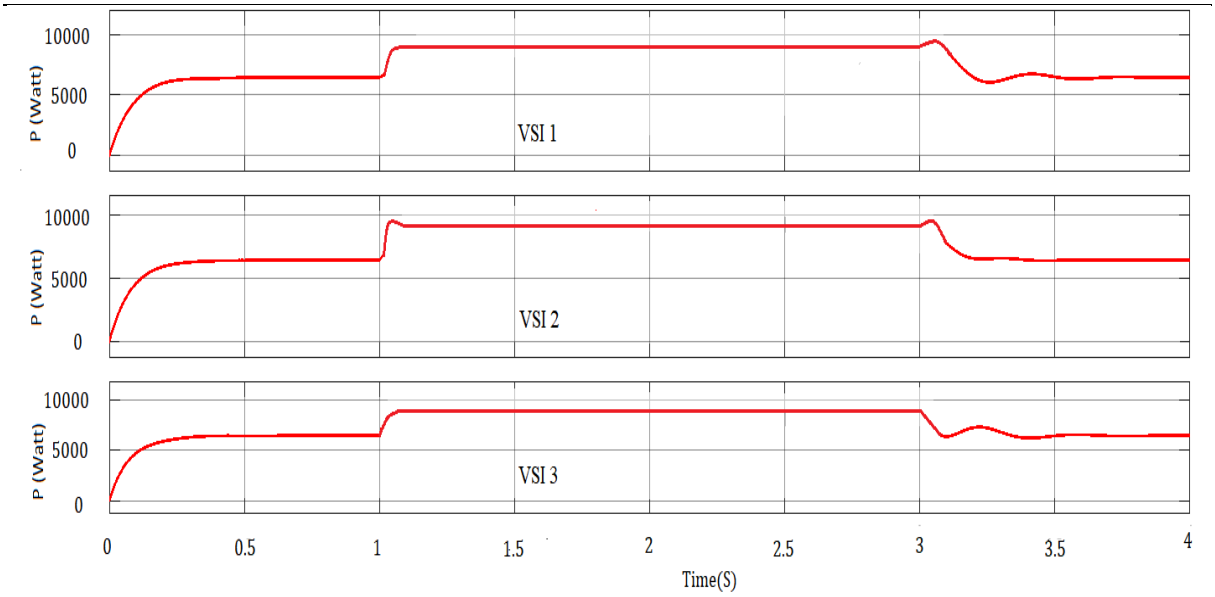

Figure 28: Active Power shared by VSI

Also, from Figure 29, it is clear that each VSI is sharing equal reactive power of 600 VAR for decreased in reactive power demand.

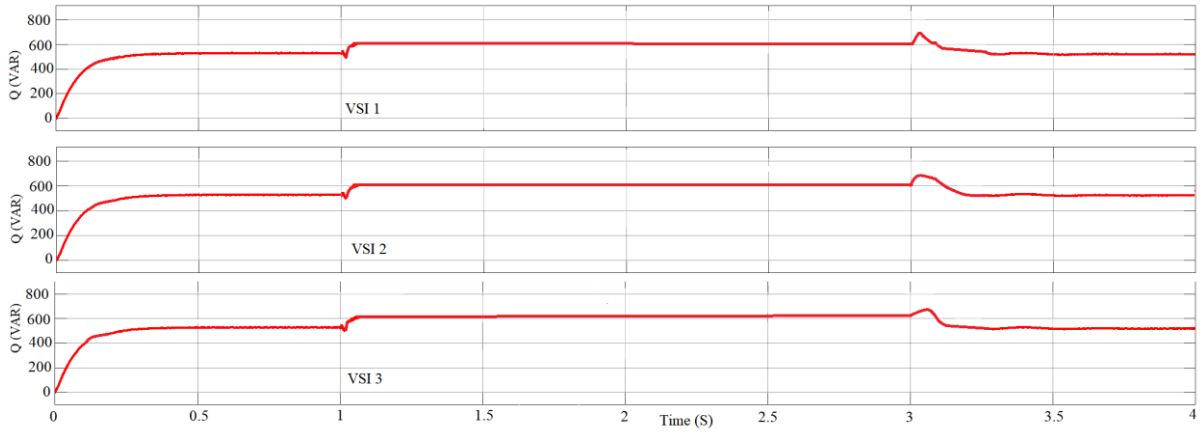

Figure 29: Reactive Power sharing by three VSI

From above it is clear that system is sharing equal active and reactive power for increased or decreased in load demand. So, it can be confirmed that system frequency and voltage are also equally deviated to meet active and reactive power demand respectively. This proves the robustness of the system.

4. Conclusions

The performance of both controllers has been analyzed and compared based on key parameters: voltage, frequency, power sharing and total harmonic distortion (THD). For linear and balanced load the conventional droop controller able to share equal active and reactive power. The system voltage is maintained at 380 V, and the current supplied by each VSI increases proportionally with added load, while the system frequency remains stable at 49.9 Hz. However, when a nonlinear and unbalanced load is introduced, power sharing becomes unequal, system voltage fluctuates up to 450 V, and THD exceeds permissible

limits, reaching 23.42% for voltage and 17.13% for current, surpassing the international standard limit of 5%.

To address these issues, the conventional droop controller was enhanced with an H-infinity controller. This modification ensured equal power sharing among VSIs, reduced system voltage fluctuations from 450 V to 400 V, maintain equal deviation in frequency for each VSI and the THD was reduced to 4.35% for voltage and 3.50% for current, bringing both within the permissible limit of 5%.

Thus, the modified droop controller using the H-infinity technique effectively mitigates the limitations of the conventional approach, enhancing power sharing, voltage and current stability, and THD compliance. These improvements demonstrate the potential of advanced control techniques in improving microgrid performance and reliability, paving the way for further research in modern power systems.

Conflicts of Interest Statement

The authors declare no conflicts of interest for this study.

Data Availability Statement

The data that support the findings of this study are available from the corresponding author upon reasonable request.

References

1. M. Abbasi, M. Hedayatpour, and A. G. Garganeev, "Microgrid voltage and frequency control using droop control based on master/slave method," in *International Conference of Young Specialists on Micro/Nanotechnologies and Electron Devices, EDM*, IEEE Computer Society, Jun. 2020, pp. 1–5. doi: 10.1109/edm49804.2020.9153493.
2. X. Hou *et al.*, "Distributed hierarchical control of AC microgrid operating in grid-connected, islanded and their transition modes," *IEEE Access*, vol. 6, pp. 77388–77401, 2018, doi: 10.1109/ACCESS.2018.2882678.
3. A. M. . Elsayed, *2017 Nineteenth International Middle-East Power Systems Conference (MEPCON) : proceedings : Electrical Engineering Department, Faculty of Engineering, Menoufia University, Egypt, 19-21 December 2017*. IEEE, 2017.
4. A. Sheela, S. Vijayachitra, and S. Revathi, "H-infinity controller for frequency and voltage regulation in grid-connected and islanded microgrid," *IEEJ Transactions on Electrical and Electronic Engineering*, vol. 10, no. 5, pp. 503–511, Sep. 2015, doi: 10.1002/tee.22113.
5. S. Sajadxan and R. Ahmad, "Model predictive control of dual-mode operations Z-source inverter: Islanded and grid-connected," in *2017 IEEE Energy Conversion Congress and Exposition, ECCE 2017*, Institute of Electrical and Electronics Engineers Inc., Nov. 2017, pp. 4971–4977. doi: 10.1109/TPEL.2017.2723358.
6. T. Hornik and Q. C. Zhong, "H∞ repetitive voltage control of grid-connected inverters with a frequency adaptive mechanism," *IET Power Electronics*, vol. 3, no. 6, pp. 925–935, Nov. 2010, doi: 10.1049/iet-pel.2009.0345.
7. T. Hornik and Q. C. Zhong, "A current-control strategy for voltage-source inverters in microgrids based on H∞ and Repetitive Control," *IEEE Trans Power Electron*, vol. 26, no. 3, pp. 943–952, 2011, doi: 10.1109/TPEL.2010.2089471.

8. Y. Shi, X. Gu, X. Yin, S. Feng, and S. Zhang, "Design of droop controller in islanded microgrids using multi-objective optimisation based on accurate small-signal model," *IET Power Electronics*, vol. 15, no. 11, pp. 1093–1109, Aug. 2022, doi: 10.1049/pel2.12293.
9. "8th ref Advanced Control Technique based on H-Infinity".
10. B. E. Sedhom, M. M. El-Saadawi, A. Y. Hatata, and E. E. Abd-Raboh, "A multistage H-infinity–based controller for adjusting voltage and frequency and improving power quality in islanded microgrids," *International Transactions on Electrical Energy Systems*, vol. 30, no. 1, Jan. 2020, doi: 10.1002/2050-7038.12143.
11. Q. C. Zhong, J. Liang, G. Weiss, C. Feng, and T. C. Green, "H∞ control of the neutral point in four-wire three-phase DC-AC converters," *IEEE Transactions on Industrial Electronics*, vol. 53, no. 5, pp. 1594–1602, Oct. 2006, doi: 10.1109/TIE.2006.882014.
12. G. Weiss, Q. C. Zhong, T. C. Green, and J. Liang, "H∞ repetitive control of DC-AC converters in microgrids," *IEEE Trans Power Electron*, vol. 19, no. 1, pp. 219–230, Jan. 2004, doi: 10.1109/TPEL.2003.820561.